

Electromagnetic Analysis Applied to the Prediction of Stray Losses in Power Transformer

L. Susnjic¹⁾, Z. Haznadar²⁾ and Z. Valkovic³⁾

¹⁾Faculty of Engineering

Vukovarska 58, 51000 Rijeka, Croatia, e-mail: livio.susnjic@riteh.hr

²⁾Faculty of Electrical Engineering and Computing

Unska 3, 10000 Zagreb, Croatia, e-mail: zijad.haznadar@fer.hr

³⁾Polytechnic of Zagreb

Konavoska 2, 10000 Zagreb, Croatia, e-mail: zvalkovi@tesla.vtszg.hr

Abstract– Flux leakage and stray losses of three-phase power transformer are analyzed using 3D-FEM with current source. The eddy current losses in the clamp plates and transformer tank are calculated in a magnetodynamic steady state load condition. Both, clamp plates and transformer tank are modeled by surface impedance method. The results are obtained at prescribed clamp plates and tank permeabilities. The influence of non-compensated ampere-turns and permeability's to the losses values are showed.

I. INTRODUCTION

Prediction of the electromagnetic phenomena in the structural metal parts in power transformer is an important step in design process to control local overheating due to leakage magnetic flux. During the past years the problem has been treated by several authors [1]-[4], mainly analyzing transformer tank losses. The authors [2] treated this problem by $\vec{T} - \Omega$ method taking into account the loss in the yoke clamp plates. The surface impedance boundary condition (SIBC) based on reduced scalar magnetic potential has been employed in [3] and [4]. The purpose of the present work is to use a 3-D finite element-based package [5] to analyze the leakage magnetic flux and stray losses due to eddy currents in the clamp plates and transformer tank. The surface impedance boundary condition based on total scalar magnetic potential has been used to represent eddy current areas.

II. MODEL

Fig. 1 shows the calculated model, whereas the tank isn't shown. The transformer main data are given in the Table I and in Fig.2. The calculation are made under the condition that the high voltage coil, the low voltage coil and the regulative coil are put into operation.

Table I Transformer Data

Quantity	Value
Rated Power	40 MVA
Frequency	50Hz
Rated Voltages, V_H/V_L	110±16% / 23 kV
Rated Currents, I_H/I_L	210/1100 A
Number of Turns $N_H/N_R/N_L$	677/120/152

The clamp plates and tank walls are made of 25 mm and 8 mm thick steel respectively, and have a conductivity of 5×10^6 S/m. The width and length of the plates are 0.423 m

and 3.8 m respectively. The magnetic core is made of M4 steel sheets.

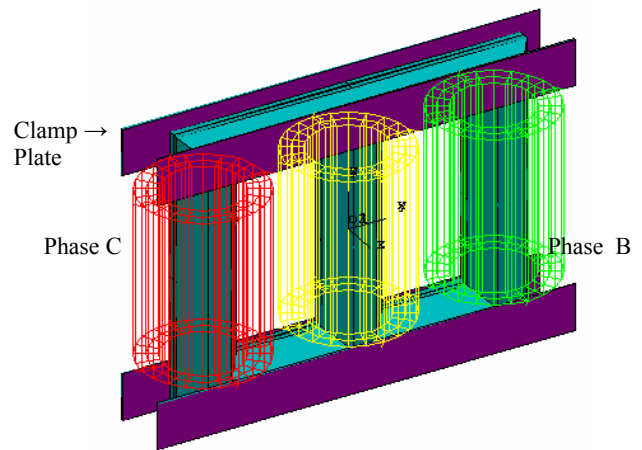


Figure 1. The calculated model (tank isn't shown).

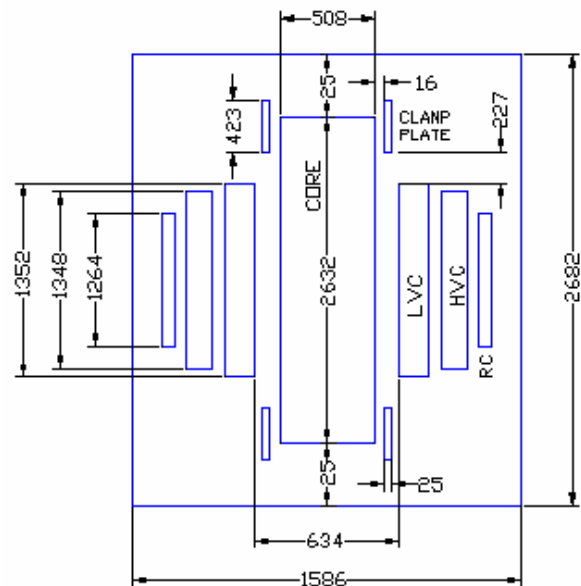


Figure 2. Geometry of the transformer cross-section.

III. METHOD OF ANALYSIS

The electromagnetic field has been calculated using a magnetodynamic model. With the exception of the coils region the sub-regions of the calculation domain are defined with total scalar potential formulation. Reduced potential described the coils region. The calculation of the magnetic field from Biot-Savart's law allows for the exclusion of the coil from finite element mesh. The nonlinearity of the main magnetic circuit is taken into account.

Surface impedance links the component of the magnetic field \vec{H} tangential to the clamping plate surface to the tangential component of the electric field \vec{E} :

$$\vec{n}x\vec{E} = Z_s \vec{n}x(\vec{n}x\vec{H}) \quad (1)$$

and for linear material is the ratio of the fundamental component of the tangential electric field E_s and the peak value of the tangential magnetic field H_s :

$$Z_s = \frac{E_s}{H_s} = \frac{1+j}{\sigma\delta} \quad (2)$$

where σ and δ are material conductivity and skin depth respectively.

Surface current density is expressed by:

$$\vec{K} = \vec{n}x\vec{H}_s \quad (3)$$

The conductor Joule loss density (surface density) in W/m² is given:

$$P=0.5 \operatorname{Re}(Z_s)|H_s|^2 \quad (4)$$

In the positive phase sequence supply conditions, a balance of the ampere-turns can be assumed for the coils wound on the same leg. The ampere-turns balanced equation in phasor form is:

$$\vec{I}_H N_H + \vec{I}_R N_R + \vec{I}_L N_L = 0 \quad (5)$$

The no load current create phase and amplitude phase shift between ampere-turns phasors in high voltage and low voltage winding. The reactive component of no load current is taken into account. The equation (5) could be rewritten:

$$\vec{I}'_L (N_H + N_R) + \vec{I}_L N_L = -\vec{I}_\mu (N_H + N_R) \quad (6)$$

Right side of the equation (6) presents non-compensated ampere-turns because of magnetizing current \vec{I}_μ . \vec{I}'_L is the low voltage winding current expressed in the primary frame of reference.

IV. RESULTS

A. VARIATIONS OF THE PHASE SHIFT BETWEEN CURRENT \vec{I}_μ AND \vec{I}'_L

For the case of phase shift between magnetizing current I_μ and current I'_L the calculated losses are given in the Table II. The relative permeability of the clamp plates and tank is fixed to 500. Loss in the clamp plates means the total loss in all four plates. It is observed that mentioned phase shift provokes non significant influence on loss values.

Table II Losses at phase shift between current \vec{I}_μ and \vec{I}'_L

Phase shift (°)	Clamp plates loss (W)	Tank loss (W)
0	3912	13352
45	3928	13402
90	3944	13146

B. PERMEABILITY VARIATIONS OF THE CLAMP PLATES, TANK RELATIVE PERMEABILITY FIXED AT $\mu_r=500$.

From table III it could be seen that clamp plates loss are slightly decreasing in relation to increasing plate's permeability. The permeability of the tank is fixed, but the influence of the clamp plate's permeability on tank loss value is evident. The higher permeability of the clamp plates provoke reduced leakage field in the tank area and as a consequence reduced tank loss. The skin depth variation is from 3.18 mm to 1mm.

Table III Losses at plate's permeability variations

μ_r of clamp plates	Clamp plates loss (W)	Tank loss (W)
100	3970	14252
200	4032	13834
300	4012	13588
400	3972	13414
500	3928	13280
600	3884	13174
700	3842	13084
800	3804	13006
900	3776	12940
1000	3732	12880

C. PERMEABILITY VARIATIONS OF THE CLAMP PLATES AND TANK

The losses calculated with simultaneously variations of the clamp plates and tank permeability are given in the Table IV. It could be seen that the clamp loss is higher for same prescribed permeability as in case B, but with lower tank permeability than in preceding case. That means that for lesser tank permeability than in case B, the value of leakage field is higher around clamp plates.

Table IV Losses at both permeability variations

μ_r of clamp plate and tank	Clamp plates loss (W)	Tank loss (W)
100	4962	12650
200	4612	13416
300	4334	13524
400	4110	13438
500	3928	13280
600	3776	13094
700	3644	12900
800	3530	12708
900	3428	12518
1000	3338	12334

Diagrams in the Fig. 3 present the clamp plates loss values computing in the case B and C.

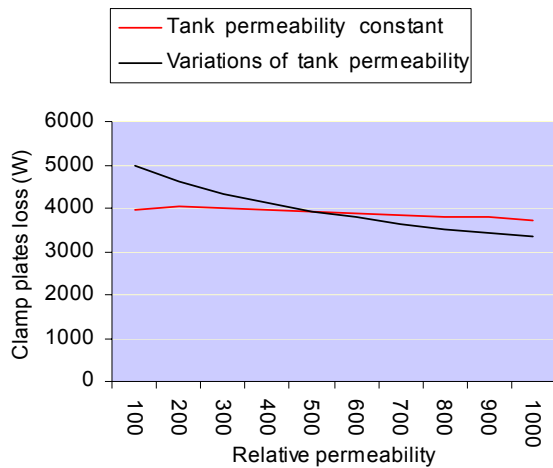


Figure 3. Clamp plates loss as function of the permeability

D. TANK REGION EXCLUDED FROM ANALYZE

Clamp plates loss is calculated also separately without taking into account the tank region. With boundary conditions of Newman type imposed on the position of the outer tank surface, obtained total loss in the clamp plates is 6528 W. With boundary conditions of Dirichlet type imposed on the position of the outer tank surface, obtained loss in the clamp plates is 2010 W.

Obtained loss values show high discrepancies with preceding cases. Therefore, tank region mustn't be excluded from analyze.

E. RESULTS FOR THE CASE A AND PHASE SHIFT OF 45°

The following results are presented for the case given in Table II with phase shift of 45°. Due to magnetizing current of 0.13 A, the number of ampere-turns in the high voltage coil and in the low voltage coil are not equal.

Fig. 4 shows distribution of the magnetic induction on the symmetry plain inside iron core and outside the core as leakage field. Distributions of power loss on the clamp plate and inner tank surface are showed in the Figs. 5 and 6, respectively. Maximum value is 2654 W/m² at front side of the plate and 1206 W/m² at tank surface. Figs. 7 and 8 show eddy currents distribution on the clamp plate and tank surface, respectively. The maximum value of the surface current density is 5427 A/m at front side of the clamp and 3006 A/m at the inner tank surface. Fig. 9 shows distribution of the tangential component of the magnetic induction on the clamp plate surface. Distribution of the magnetic induction absolute value on the inner tank surface is shown in Fig. 10. Distribution of the normal component of the magnetic induction on the clamp plate surface is shown in Fig. 11.

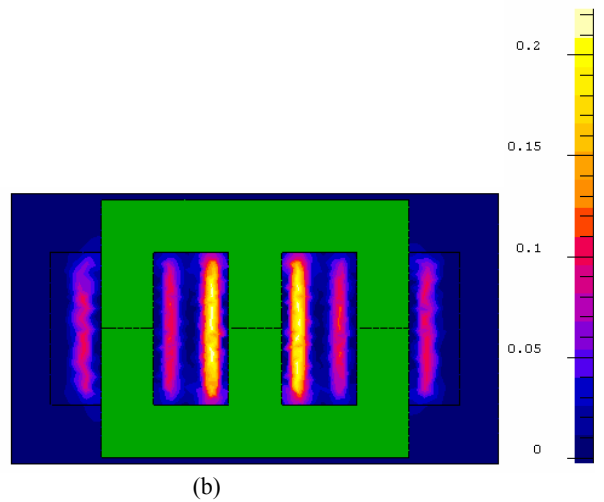
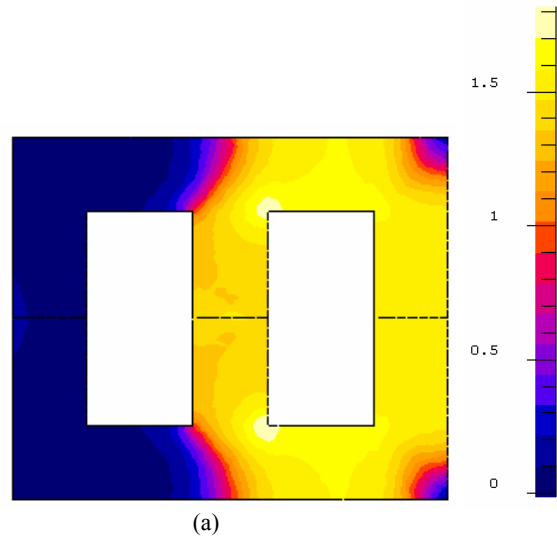
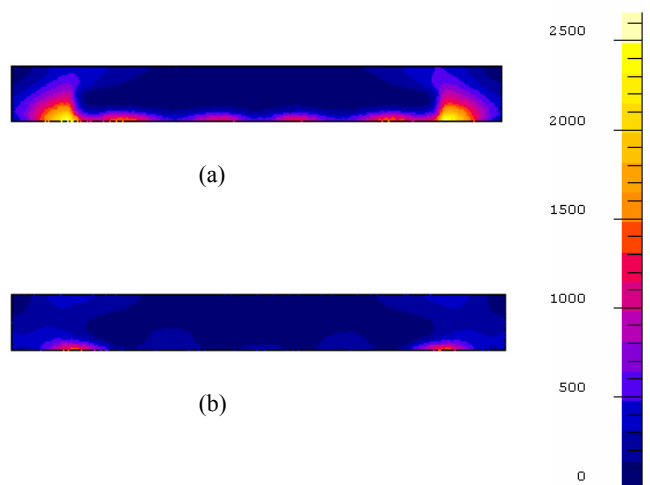
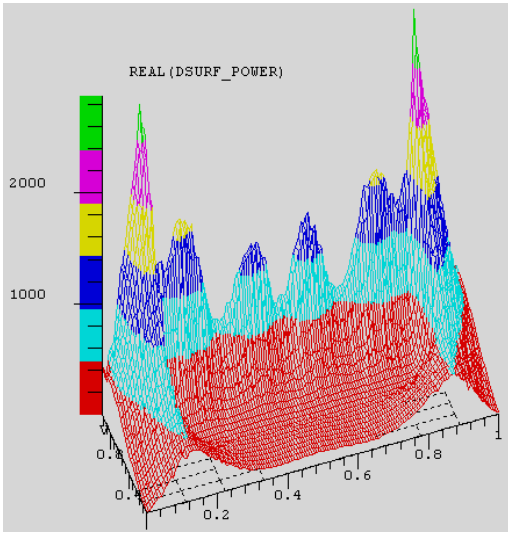


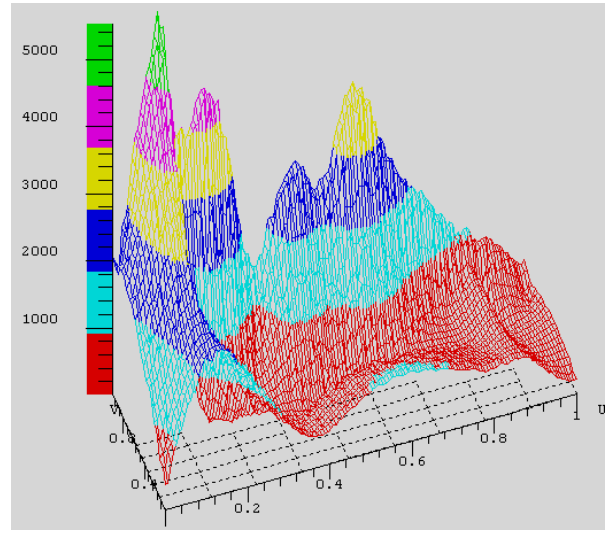
Figure 4. Distribution of magnetic induction at instant $\omega t=0^\circ$, (T). (a) on the core surface - symmetry plain, b) (leakage field) on symmetry plain.





c)

Figure 5. Power losses distribution on the clamp plate surface (W/m^2). (a) isovalue-front side, (b) isovalue - back side, (c) front side-spatial diagram.



(c)

Figure 7. Eddy current distribution on the clamp plate (A/m). (a) isovalue-front side, (b) isovalue - back side, (c) front side-spatial diagram.

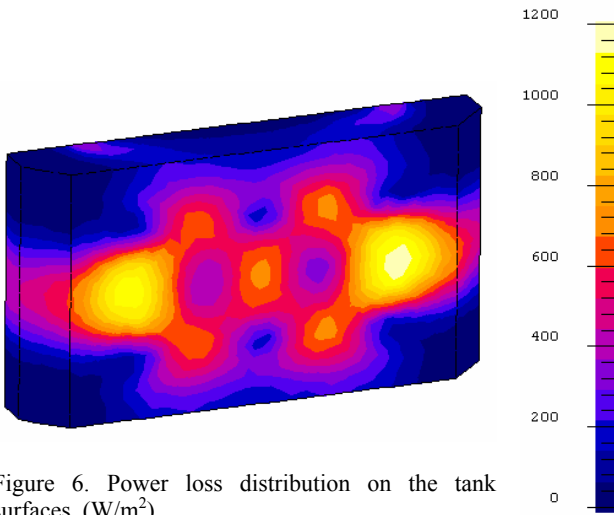


Figure 6. Power loss distribution on the tank surfaces (W/m^2).

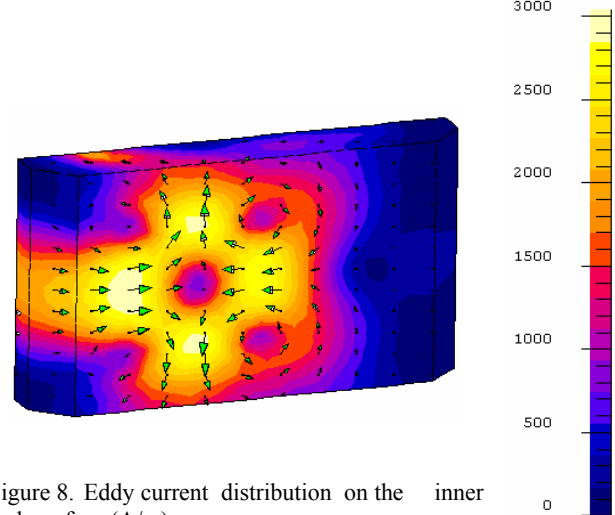
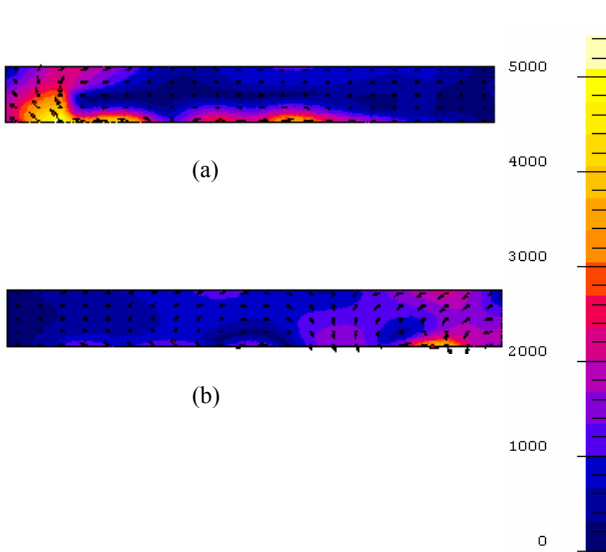
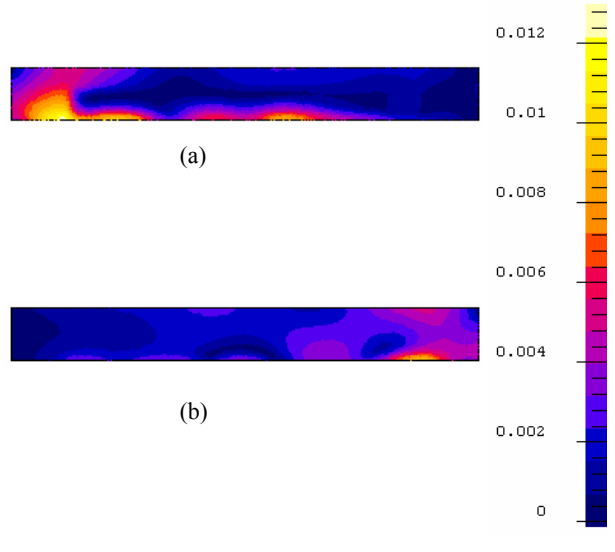


Figure 8. Eddy current distribution on the inner tank surface (A/m).



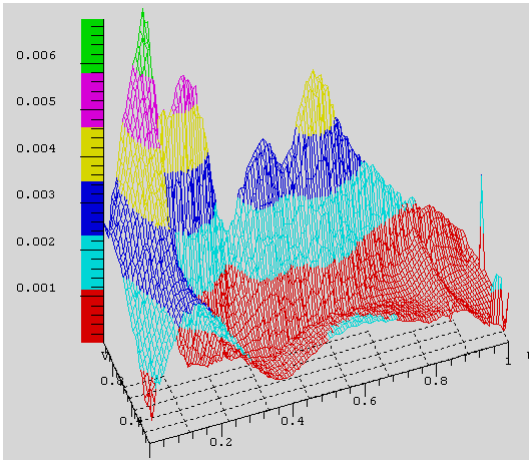
(a)

(b)



(a)

(b)



(c)

Figure 9. Distribution of magnetic induction tangential component on clamp plate surface (T). (a) isovalue-front side, (b) isovalue - back side, (c) front side-spatial diagram.

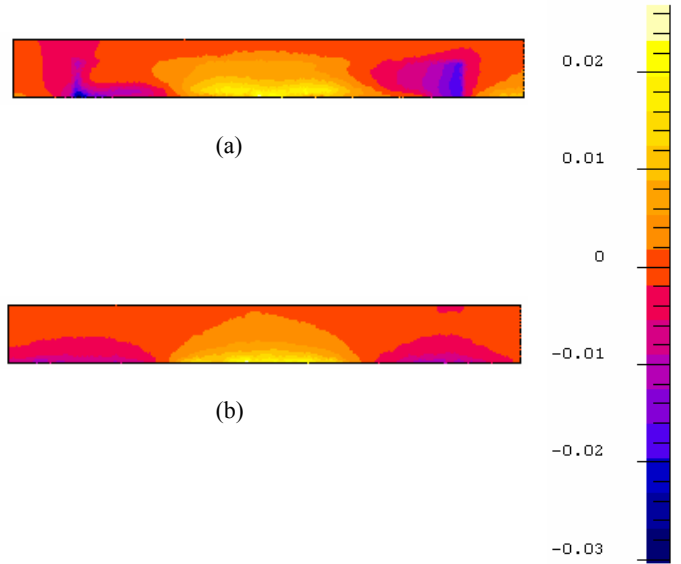


Figure 11. Distribution of magnetic induction normal component on clamp plate surface (T). (a) isovalue-front side, (b) isovalue - back side.

V. CONCLUSION

The losses effect of induced eddy current in the transformer clamp plates and unshielded tank walls have been computed. The obtained results showed that power loss in the clamp plates depend simultaneously on the loss and the tank permeability. Similar conclusion can be valid for tank loss. The phase shift between magnetizing current and secondary current showed no significant influence on losses values. The experimental proof of calculation is difficult to realize. The comparison with calculation may come from industrial experiences.

REFERENCES

- [1] Rizzo M., Savini A., Turowski J., "Influence of Flux Collectors on Stray Losses in Transformers"; *IEEE Trans. of Magnetics*, Vol. 36, No.4, pp. 1915-1918, July 2000.
- [2] T. Renyuan, L. Yan, L. Feng, T. Lijian, "Resultant Magnetic Fields due to Both Windings and Heavy Current Leads in Large Power Transformers"; *IEEE Trans. of Magnetics*, Vol. 32, No.3, pp. 1641-1644, May 1996.
- [3] Sakellaris J., Meunier G., Brunotte X., Guerin C. and J.C. Sabonnadiere., "Application of the impedance boundary condition in a finite element environment using the reduced potential formulation"; *IEEE Trans. of Magnetics*, Vol. 27, No.6, pp. 5022- 5024, November 1991.
- [4] Guerin C., Meunier G., "Surface Impedance for 3D Non-linear Eddy Current Problems - Application to Loss Computation in Transformers"; *IEEE Trans. of Magnetics*, Vol. 32, No.3, pp. 808-811, May 1996.
- [5] FLUX V.8.1, "CAD package for electromagnetic and thermal analysis using finite elements", CEDRAT, October 2003.

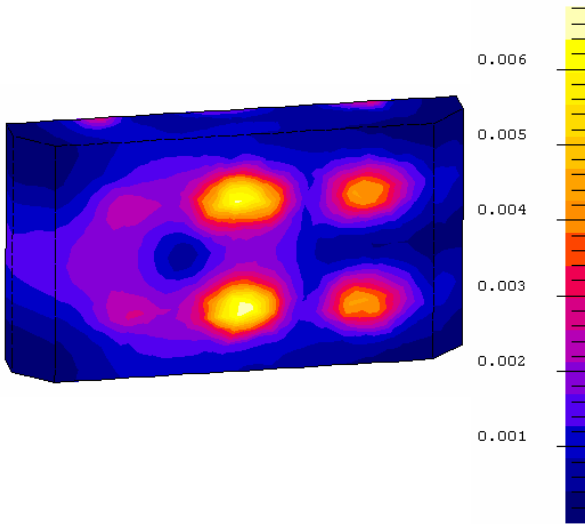


Figure 10. Distribution of magnetic induction on clamp plate surface (T).

The maximum obtained magnetic flux density (tangential component) of 6 mT is less than the critical overheating criterion value of 26 mT [2] and therefore no local overheating in the clamp plates would be present.